Journal of Environmental Management 356 (2024) 120628

Contents lists available at ScienceDirect

Journal of Environmental Management

journal homepage: www.elsevier.com/locate/jenvman

Research article

UV/TiO_2 photocatalysis as post-treatment of anaerobic membrane bioreactor effluent for reuse

Yu Huang [1], Paul Jeffrey, Marc Pidou [*]

Cranfield Water Science Institute, Cranfield University, Cranfield, MK430AL, United Kingdom

ARTICLE INFO

Handling editor: Raf Dewil

Keywords:
UV
TiO_2
Anaerobic
Membrane bioreactor
Adsorption
Nutrients

ABSTRACT

Advanced oxidation processes have been widely applied as a post-treatment solution to remove residual organic compounds in water reuse schemes. However, UV/TiO_2 photocatalysis, which provides a sustainable option with no continuous chemical addition, has very rarely been studied to treat anaerobically treated effluents. In the current study, the removal of organics and nutrients from an anaerobic membrane bioreactor (AnMBR) effluent is evaluated during adsorption and photocatalysis processes under various conditions of TiO_2 dose and UV intensity and compared to the effluent from an aerobic membrane bioreactor (AeMBR). The sequence for preferential adsorption on TiO_2 was found to be phosphorus, inorganic carbon and then ammonia/organic carbon were found. The competing effect between the organics and nutrients, along with the low UV transmission efficiency caused by the need for high doses of TiO_2, ultimately compromise the organic removal efficiency in the AnMBR permeate. TiO_2 dosage was found to have a greater impact than UV intensity on improving the overall removal performance as nutrients are competing for the adsorption site but are not photodegraded. Under the same operational condition, the UV/TiO_2 photocatalysis displayed a higher removal efficiency of organic matter and phosphorus in the AeMBR effluent due to a lower initial organics concentration and absence of ammonia as compared to the AnMBR effluent.

1. Introduction

Global water scarcity has led to the pursuit of sustainable and safe water sourced from treated wastewater (Lazarova, 2015; Salgot and Folch, 2018). Advanced treatment technologies, such as reverse osmosis (RO) membranes, ion exchange (IEX), as well as advance oxidation processes (AOPs) have been widely applied to tackle the residual fractions of organic compounds in the secondary effluent from conventional wastewater treatment trains (Rebelo et al., 2018; Salgot and Folch, 2018; Tang et al., 2018). However, organic contaminants that present a neutral charge or have a low molecular weight (molecular size <300 Da) are poorly removed by the RO and IEX (Finkbeiner et al., 2018; Mangalgiri et al., 2019), some of which have been reported to cause endocrine and toxicological responses in human cells (Li et al., 2018). In contrast, AOPs are extensively proven as effective tools to remove the excess organic compounds in particular for water reuse applications, with numerous studies evidencing a successful elimination of organic micro pollutants (OMPs), including pesticides and pharmaceuticals (Kanakaraju et al., 2018; Suzuki et al., 2015; Villegas-Guzman et al., 2017). In various evidenced AOPs, heterogeneous photocatalytic systems are widely reported as more sustainable and effective over homogeneous-phase options (Atalay and Ersöz, 2020; Villegas-Guzman et al., 2017). In particular, titanium dioxide (TiO_2), has been reported as a physically robust and relatively nontoxic material (Levchuk and Sillanpää, 2020), with inexpensive overall operation cost due to the regenerable catalyst and applicable solar power (Loeb et al., 2019).

Anaerobic membrane bioreactors (AnMBRs) offer the potential of treating municipal wastewater with a lower footprint, energy neutrality, and less waste sludge production (Shin and Bae, 2018; Song et al., 2018a). However, AnMBRs deliver limited organic removal performance under operating conditions such as low hydraulic retention time (HRT) (Chen et al., 2015; Mei et al., 2017) or psychrophilic temperatures (Crone et al., 2016; Dolejs et al., 2017). Although, the effluent quality achieved can meet standards for discharge, this can result in an inadequate effluent quality to meet the stricter organic parameter threshold in reuse standards (Augsburger et al., 2021; Foglia et al.,

* Corresponding author.
E-mail address: m.pidou@cranfield.ac.uk (M. Pidou).
[1] Present address: Yunnan Provincial Key Laboratory of Soil Carbon Sequestration and Pollution Control, Faculty of Environmental Science & Engineering, Kunming University of Science & Technology, Kunming 650,500, China.

https://doi.org/10.1016/j.jenvman.2024.120628
Received 16 October 2023; Received in revised form 5 February 2024; Accepted 10 March 2024
Available online 22 March 2024

2019). Furthermore, as nutrients (ammonia and phosphorus) are not removed in AnMBRs, there are concerns about their ability to deliver in the context of high grade water reuse applications such as groundwater recharge or surface water augmentation (CNEPA, 2021; Harb and Hong, 2017; USEPA, 2017). For discharge and more importantly reuse, the AnMBR effluent typically will require a post-treatment process to eliminate the residual organic fraction including trace micropollutants and possibly nutrients (CNEPA, 2021; ISO, 2018; USEPA, 2017, 2012). In these regards, photocatalytic TiO_2 offers a promising post-treatment solution for AnMBR effluent through adsorption and elimination of organic matter and ammonia (Lee et al., 2002; Maghsoodi et al., 2019; Snow et al., 2019; Zhang et al., 2021), while adsorbing the phosphorus (Lee et al., 2016), to potentially achieve a high effluent quality and resource recovery for water reuse implementations.

Existing literature has largely focused on the post-treatment of effluents from aerobic biological systems but with relatively few studies specifically on aerobic membrane bioreactor (AeMBR) effluents. Interestingly, the combination of AeMBR + UV/TiO_2 has been shown to produce an effluent quality sufficient for recycled greywater for toilet flushing with a high removal of major pharmaceuticals (Ojobe et al., 2021) while achieving a higher oxidation rate for selected pharmaceuticals in comparison to photo-Fenton, UV/Fe and UV/H_2O_2 (Benitez et al., 2011). However, it is critical to know that unremoved organic matter can inhibit the photocatalytic process through hindering photocatalytic formation of $OH^{\cdot}$ radicals by particle aggregation (Janssens et al., 2019), or extinguish the sorption onto the TiO_2 surface hence no reaction with surface bound $OH^{\cdot}$ radicals (Maghsoodi et al., 2019). as Also, it can lead to a decrease in the affinity of dissolved organic matter (DOM) to the catalyst surface (Snow et al., 2019), which ultimately leads to a strong quenching effect of reactive oxygen species (ROS). Overall, there is strong evidence in the literature that the water matrix has a significant impact on the degradation and mineralization efficacy by affecting the compound adsorption, surface radical generation and UV transmission efficiency (Kanakaraju et al., 2018; Levchuk and Sillanpää, 2020; Snow et al., 2019; Villegas-Guzman et al., 2017). Our previous work with AnMBR and AeMBR pilot systems has shown a clear difference in organic removal and nitrogen species between the two effluents, where the COD and DOC of the AnMBR effluent was 2–4 times higher than AeMBR effluent, while ammonia and nitrate were the unique nitrogen forms in the AnMBR and AeMBR effluents, respectively (Huang et al., 2023). As such, this suggests that a different behaviour can be expected when treating anaerobically treated effluent with TiO_2/UV. but there is to date very limited literature on the application of AOPs as the post-treatment step for AnMBR effluent. Augsburger et al. (2021) proposed that UV/H_2O_2 can be the final polishing and disinfection process while avoiding additional steps for the removal of nutrients, producing a high-quality effluent as liquid fertilizer for crops production. However, no study has investigated the potential application of UV/TiO_2 as the post-treatment for AnMBR effluent.

The current study then reports the first investigation of the application of UV/TiO_2 to an AnMBR effluent, to understand the impact of operational conditions and nutrient content on the photocatalysis process for the post-treatment of AnMBR effluent for reuse. The removal of organic matter and nutrients in the AnMBR effluent is evaluated during the adsorption and photocatalysis processes, under various TiO_2 doses and UV intensities with a direct comparison to an AeMBR, to evaluate the potential to achieve sufficient effluent quality and effective large-scale applications for sustainable water recycling.

2. Materials and methods

2.1. Pilot scale AnMBR and AeMBR

AnMBR and AeMBR pilot plants were installed at Cranfield University's National Research Facility for Water and Wastewater. The systems were fed with settled municipal wastewater from the Cranfield University sewage works after settling in a primary settling tank. Details about the MBRs can be found in Huang et al. (2022). Effluents used in adsorption and photocatalytic tests were sampled simultaneously from the AnMBR and AeMBR to minimize the effect on the effluent matrix caused by variation of influent wastewater. Characterization of the effluents is listed in Table 1.

2.2. TiO_2 adsorption tests

A standard TiO_2 nano powder (CAS: 13,463-67-7) with a 21 nm primary particle size and ≥99.5% trace metals basis was obtained from Sigma-Aldrich (Merck, USA). Under dark conditions, 500 ml samples of MBR effluent were stabilized to room temperature (20 °C) then transferred to a 1L beaker (Fisher scientific, UK) to which the TiO_2 was added. A constant 400 RPM stirring rate was maintained with a magnetic stirrer (Benchmark 3770, UK) to mix the TiO_2 powder within the MBR effluents. Prior to the adsorption test, blank tests were carried out with no TiO_2 addition to the AnMBR and AeMBR effluent. Adsorption isotherm tests were conducted with TiO_2 dosing concentrations of 0.1, 0.2, 0.5, 1, 2 and 5 g/L. The TiO_2 concentrations, test duration and sampling intervals were all chosen based on previous trials reported for wastewater (Lofrano, G., Libralato, G., Casaburi, A., Siciliano, A., Iannece, P., Guida, M., Pucci, L., Dentice, E.F., Carotenuto, M., n.d.. n.d.. Municipal wastewater spiramycin removal by conventional treatments and heterogeneous photocatalysis (2018). Science of the Total Environment 624, 461–469. doi:10.1016/j.scitotenv.2017.12.145.; Rivero et al., 2006; Tsoukleris et al., 2023). A 15 ml sample was taken from the beaker with a syringe at regular intervals over the duration of the tests to monitor the adsorbate concentration. Adsorption isotherms were described with the Langmuir isotherm (Equation (1)), Freundlich isotherm (Equation (2)) and a normalised Freundlich isotherm (Li et al., 2002) (Equation (3)).

$$\frac{1}{q}=\frac{1}{q_m}+\frac{1}{bq_mC_e} \tag{1}$$

$$log\ q = log\ K_f + \frac{1}{n} log\ C_e \tag{2}$$

$$q = K_f^{'}\left(\frac{C_e}{D_0}\right)^{\frac{1}{n}} \tag{3}$$

Where, q (mg/g) is the amount of material adsorbed per unit weight of adsorbent, C_e is the concentration of material remaining in the solution (mg/L). In equation (1), b and q_m are constants. These constants can be determined by plotting $\frac{1}{q}$ vs $\frac{1}{C_e}$; While in equation (2), K_f and n are the Freundlich parameters which can be determined by plotting $\log C_e$ against $\log q$; and in equation (3), D_0 represents the dose of adsorbent which is applied to normalize the remained concentration.

Table 1
Characterization of AnMBR and AeMBR effluents fed to the photocatalytic reactor.

Parameter	AnMBR		AeMBR	
mg/L	Mean	Std	Mean	Std
pH	7.22	±0.1	7.29	±0.1
TSS	ND		ND	
Coliforms*	ND		ND	
COD	68	±5.5	18	±3.5
DOC	28.02	±2.8	6.75	±1.3
NH_4–N	43.96	±3.1	ND	
NO_3–N	ND		33.02	±2.4
TN	44.56	±3.5	33.09	±2.5
PO_4–P	6.91	±0.2	5.22	±0.3
TP	6.91	±0.2	5.22	±0.3

Notes: Std: Standard Deviation. Coliforms*: Faecal, Escherichia and total coliforms. ND: Non detectable.

2.3. UV/TiO_2 photocatalysis tests

UV assisted photocatalysis batch tests were conducted with a lab-scale quasi-collimated beam apparatus (Herford, Germany) equipped with three monochromatic low-pressure UV-C (254 nm) lamps placed in a dark room. The UV irradiance was determined as 30, 40 and 50 W/m^2 with the correspondence distance between the lamps and the petri dish of 17, 12 and 8 cm, respectively. The detailed system setup can be obtained from Carra et al. (2016).

Under dark conditions, room temperature MBR effluent was transferred to a 250 ml petri dish and placed on a magnetic stirrer (Benchmark 3770, UK) under the UV lamps. The mixing of the TiO_2 powder and the solution was maintained by a 5 cm long magnetic stirring bar (Fisher scientific, UK) with a constant 400 RPM stirring rate to overcome the reduction of the photocatalysis efficiency caused by the poor mixing of the solution reported in Carra et al. (2016). Each test was done in duplicate with a total irradiance time of 300 min, a 15 ml monitoring sample was taken from the centre of the petri dish at the reaction times of 10, 30, 60, 120, 180, 240 and 300 min. To calibrate the change in concentration caused by temperature increase from UV radiation, an evaporation coefficient was calculated with the TN concentration measured during the UV/TiO_2 photocatalysis of the AeMBR effluent since there was no TN removal observed. The coefficients for 30, 40 and 50 W/m^2 were calculated as a function of the respective UV irradiation intensity, then applied to each measured parameter under the same intensity for both AnMBR and AeMBR samples. A summary of the test conditions is reported in Table 2.

The photocatalytic process for organic matter and nitrogen was described with a pseudo first order expression (Equation (4)) and the adsorption process for phosphorus was described by a pseudo second order kinetic model (Equation (5)) which has been widely applied in documented literatures (Carra et al., 2016; Lee et al., 2016; Li et al., 2008; Murgia et al., 2005).

$$ln\frac{C_0}{C_e} = k_1 t \tag{4}$$

$$\frac{t}{q_t} = \frac{1}{k_2 q_e^2} + \frac{t}{q_e} \tag{5}$$

Where in equation (4), C_0 (mg/L) is the initial concentration of material in the solution, C_e (mg/L) is the concentration of material remaining in the solution at t time, k_1 is the rate constant of pseudo first order kinetic, and t (min) is the time consumed; while in equation (5), k_2 (g/mg·min^{-1}) is the rate constant of pseudo second order kinetic, q_t and q_e (mg/g) are the adsorption capacity at time t and at equilibrium, respectively.

2.4. Analytical measurements

Chemical oxygen demand (COD), ammonia nitrogen (NH_3–N), nitrite (NO_2–N), nitrate (NO_3–N), phosphate (PO_4–P), and total phosphorus (TP) were analysed with cell tests and a photo spectrometer (Merck Spectroquant, Germany). Dissolved organic carbon (DOC) and total nitrogen (TN) were measured by a Shimadzu TOC analyser (Shimadzu 3201, Japan). Characterization of the samples was undertaken after filtering with 0.45 μm syringe membrane disc filter (Merck Millipore, Germany) to remove the TiO_2 particles. Although the TiO_2 primary particle size is 21 nm, it has been shown to aggregate to form larger particles when dispersed in water (Pidou et al., 2009) and hence will be removed by a 0.45-μm filter. Organic composition was evaluated by a fluorescence spectrometer (HORIBA FLuoroMax+, Japan) with a 3D excitation–emission matrices. Scan settings were 200–400 nm excitation and 280–500 nm emission wavelength, 1 nm entrance slit and an integration time of 0.1 s. The 1st and 2nd Rayleigh scatter was masked with 5 nm slit width by FluorEssence software (HORIBA, Japan). The fluorescence integrated composition analysis was extracted with as described in Huang et al. (2022).

Table 2
UV/TiO_2 test scheme for this study.

Batch	Effluent	sTiO_2 dosage (g/L)	UV intensity (W/m^2)
1	AnMBR	0.5	30, 40, 50
	AeMBR	1	30, 40, 50
		2	30, 40, 50
2	AnMBR	5	30
		10	

3. Results and discussion

3.1. TiO_2 adsorption isotherms

No DOC or TN reduction was observed in the blank test for the AnMBR and AeMBR effluents confirming that any removal observed in the presence of TiO_2 can be attributed to adsorption on the media. Limited DOC adsorption (<20%) was found in all AnMBR (Fig. 1a) and AeMBR (Fig. 1d) effluent samples even when the TiO_2 dose was increased. Also, no clear correlation was observed between the adsorption performance and the TiO_2 dose in both MBR effluents. For the test with 2 g/L TiO_2 over an extended period (33 h) (Fig. 1a), the DOC concentration was found to first decrease, demonstrating some adsorption before increasing back to just over the initial concentration ($C_e/C_0 = 1.05$) suggesting a desorption and release back into solution. It should be noted that the dissolved organic carbon (DOC) is calculated as the difference between the total carbon (TC) and inorganic carbon (IC) and, interestingly, the removal profiles of TC (Fig. 1b and 1e) and IC (Fig. 1c and 1f) for the two effluents displayed a distinguishable removal linked to the TiO_2 dosing concentration. This can be explained by the fact that the high molecular weight (MW) carbon substances have a higher adsorption potential by TiO_2 (Benkoula et al., 2015; Thomas and Syres, 2012). Our previous work has suggested that the organic matter matrix is similar in the two effluents with a high content of humic acid-like substances (Huang et al., 2022), while the size distribution results displayed a negligeable difference in Dv50 (size point below which 50% of the material is contained) between all samples with the same TiO_2 doses (n = 10). Since the initial TC and IC concentrations in the AnMBR effluent were more than 4 times higher than for the AeMBR effluent, this suggests that the IC compounds in both effluents consist of high MW substances, while in contrast the other fraction of the TC has low MW. This variation leads to different adsorption rates in the isotherms and may ultimately lead to a different degradation rate during the photocatalysis process of the DOC and IC.

No TN adsorption was identified in any of the AeMBR samples, while for the AnMBR, all TN adsorption profiles displayed a similar adsorption rate and capacity irrespective of the TiO_2 dose. The longer adsorption test with a 2 g/L TiO_2 dose in the AnMBR effluent did not reach equilibrium while keeping the same adsorption rate (Fig. 1g). Noticeably, the AnMBR effluent only exhibited a 0.15 ± 0.1 increase over the initial pH (7.22), suggesting there is no ammonia volatilization since the main fraction was ammonium under this pH and temperature (20 °C) (Shin et al., 2021; Venkiteswaran et al., 2019). This is further supported by the fact that no removal of ammonium was recorded in the blanks. Moreover, the unreached equilibrium observed for TN in the AnMBR effluent can be explained by the triple bound adsorption of ammonium ions on the TiO_2 surface in the presence of H_2O ions (Markovits et al., 1996), which leads to the largest capacity observed over other adsorbates. For TP adsorption, the profiles of both effluents displayed a strong increasing adsorption rate and overall capacity with increasing TiO_2 dosage (Fig. 1h and 1i), which agrees with Lee et al. (2016) that increasing the TiO_2 dosage can affect the overall adsorption capacity of phosphorus. The adsorption of phosphate is evidenced to turn the zeta potential of the water dispersed TiO_2 surface from positive to negative

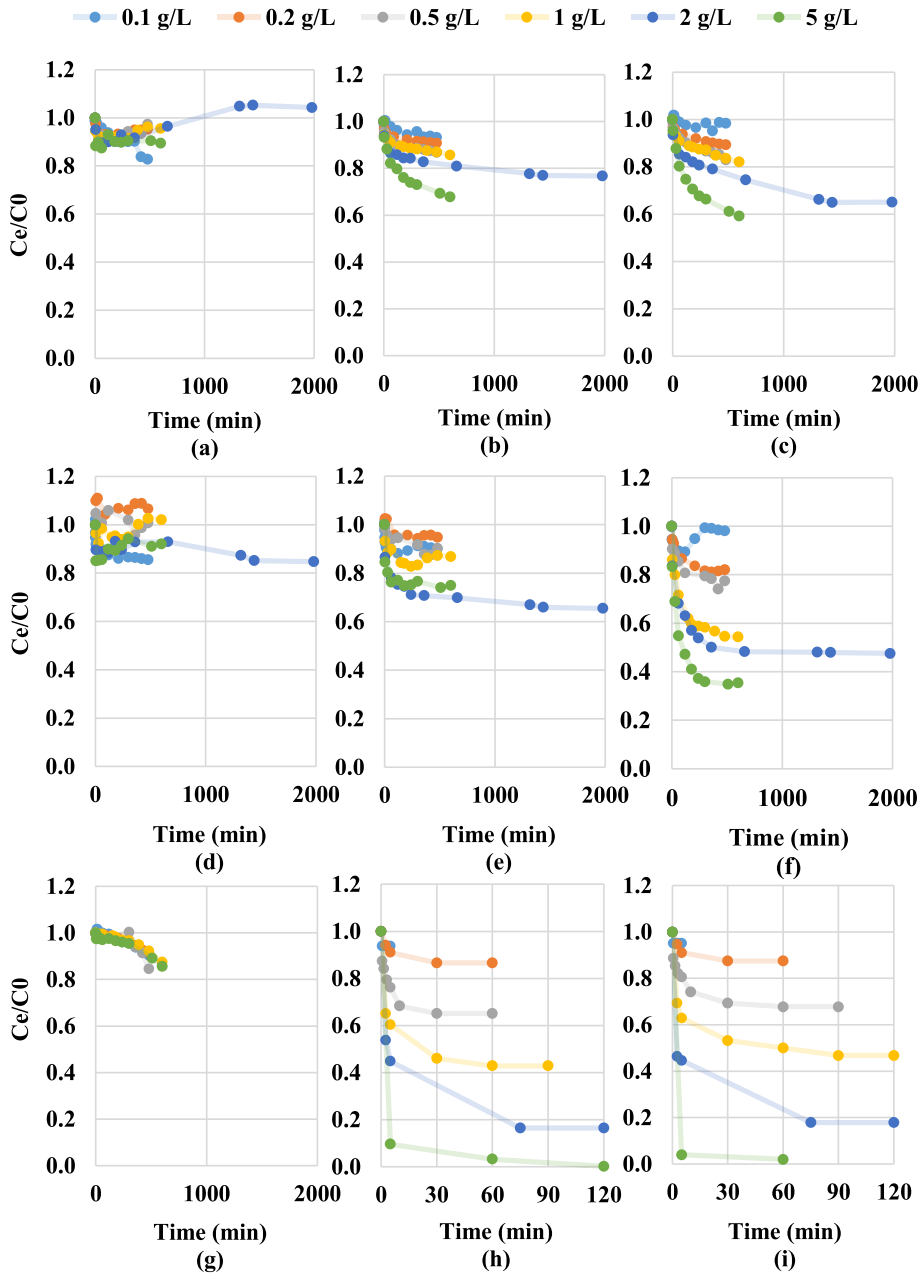

Fig. 1. Adsorption profiles of various compounds in AnMBR (DOC-a, TC-b, IC-c, TN-g, TP-h) and AeMBR (DOC-d, TC-e, IC-f, TP-i) effluents for varying doses of TiO_2 between 0.1 and 5 g/L.

(Domingos et al., 2010; Halimi et al., 2014), causing a charge neutralisation effect with the positively charged ammonium, as the adsorption of both ammonia and phosphate in the AnMBR effluent is enhanced. Therefore, this explains the slightly higher TP removal observed for AnMBR sample compared to that in the AeMBR sample conducted with the same TiO_2 dosage, but ultimately, this will reduce the adsorption capacity of the organics by taking the limited adsorption site on the TiO_2 surface. Hence the different nitrogen adsorption behaviour was caused by a different form of nitrogen in the two effluents; in the form of ammonium in the AnMBR effluent and nitrate in the AeMBR effluent. However, the adsorption of the ammonia exhibited a completely different behaviour among all measured compounds as the adsorption capacity was not affected by the TiO_2 concentration. There is no clear explanation for this phenomenon and no evidence of a similar behaviour has been reported in the literature so further specific research may be needed for the mechanism to be fully explained.

The corresponding isotherm parameter $K_f^{'}$ for all adsorbents displayed in Fig. 2 were obtained with the normalised Freundlich isotherm as it presented the highest overall coefficient of determination value (R^2) among the three models applied (Table S1, Supplementary material). DOC was excluded due to poor correlation ($R^2 < 0.3$) observed in all fittings, therefore the displayed $K_f^{'}$ are for TC, IC, TP and TN (AnMBR only) with an average R^2 of 0.9/0.6, 0.9/0.9, 0.9/0.9 and 0.9, for the AnMBR and AeMBR samples, respectively.

As $K_f^{'}$ reveals the adsorption capacity for the compound per unit mass of dosed TiO_2, this can provide an indication of adsorption efficiency at the corresponding dose. The $K_f^{'}$ value for TC and IC from the AnMBR effluent displayed an obvious variation at each TiO_2 dose, with the lowest $K_f^{'}$ observed for the lowest (0.1 g/L) and the highest (5 g/L) doses. The low $K_f^{'}$ value obtained for the low dose is due to the limited overall

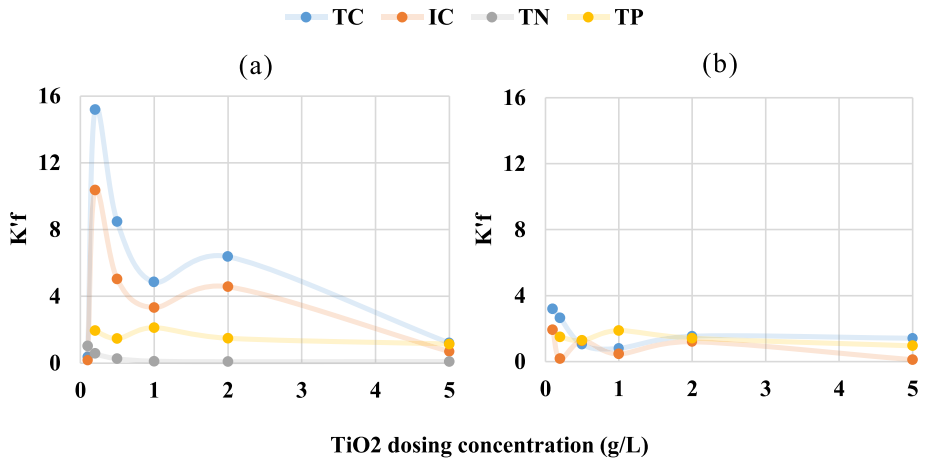

Fig. 2. $K_f^{'}$ of each adsorbent from the normalised Freundlich isotherms for the AnMBR (a) and AeMBR (b) effluents.

adsorption capacity, while the low $K_f^{'}$ value at the high dose is due to the limited increase in $K_f^{'}$ once the adsorbate reached equilibrium as the residual concentration in the samples remain stable. This result agrees with Li et al. (2002) who showed that the adsorption capacity is less affected by increasing the adsorbent dosage in high initial adsorbate concentration solutions, which in this case is the AnMBR effluent. The slight increase in $K_f^{'}$ for TC and IC in the test at 2 g/L TiO_2 can be explained by the fact that the duration of this specific test was extended and further removal occurred (Fig. 1b and c) hence affecting the overall capacity. In contrast, the AeMBR samples displayed much less variation with similar $K_f^{'}$ values regardless of the dosed amount. Indeed, the $K_f^{'}$ values for TC and IC for the AnMBR effluent were higher than for the AeMBR effluent with TiO_2 doses of 0.2, 0.5, 1, and 2 g/L. This agrees with the findings reported in the literature that a higher unit adsorption capacity is expected in the more concentrated solution under the same adsorbent dose (Lim et al., 2011; Thomas and Syres, 2012). Indeed, the $K_f^{'}$ values for TC and IC were 15.2 and 10.4 in the AnMBR effluent with 0.2 g/L TiO_2, which is significantly higher in comparison to the corresponding values of 2.6 and 0.18 for the AeMBR effluent.

Despite the different initial concentration, the nitrogen species produced by the different biological stages of two MBRs also impact differently on the adsorption of organics. The ammonium in the AnMBR effluent could have a charge interaction effect with phosphate, competing for the available adsorption site on the TiO_2 surface, which leads to a decreased adsorption capacity for the organics. Whilst nitrate has been shown to decrease NOM adsorption on TiO_2 (Gora and Andrews, 2017), along with the competing effect from phosphate, this explains the significantly lower $K_f^{'}$ found for the AeMBR effluent even with a much lower initial compounds concentration compared to AnMBR effluent. Furthermore, since the performance of the photocatalysis process is influenced by the adsorption rate (Azeez et al., 2018; Levchuk and Sillanpää, 2020), this suggests a different organic removal performance should also be expected in the photocatalysis tests.

The higher $K_f^{'}$ for TP compared to TN in the AnMBR effluent confirmed the charge neutralisation effect between the ammonium and phosphate. A similar $K_f^{'}$ of TP was observed in both MBR effluents when the same dose was applied. This confirmed these two effluent matrices had a negligible impact on the adsorption mechanism of the phosphorus compound, but may suggest there is no optimum TiO_2 dosing ratio for the MBR effluents to prioritise for phosphorus adsorption. However, phosphate reached an adsorption equilibrium within the shortest time compared to the other substances, suggesting that phosphate has the highest adsorption rate due to a higher MW and a positive charge compared to other compounds in the effluent. As there is no evidence reported in the literature of the photodegradability of phosphate by UV/TiO_2, this may be a cause for concern for the application as the overall photocatalysis efficiency will be reduced when phosphate occupy adsorption sites on the surface of the TiO_2 but is not removed photocatalytically. The adsorption priority of each compound is concluded to be as phosphorus - inorganic carbon - ammonia/organic carbon in the AnMBR effluent, whilst phosphorus - inorganic carbon - organic carbon in the AeMBR effluent.

3.2. *UV/TiO_2 photocatalysis performance*

It should first be noted that there was no removal of DOC, TN and TP from either MBR effluent with direct UV photolysis. Notably, the pH value in all samples showed a minor change (<0.1) after the addition of TiO_2 but remained stable during the whole progress of the photocatalysis process, hence volatilization was not considered as a pathway for ammonia removal from the AnMBR effluent.

3.2.1. *Removal of bulk organic and nutrients*

The DOC removal profile of the AnMBR effluent exhibited significant variations corresponding to changes in TiO_2 dose and UV intensity (Fig. 3a). The relative linearity of these profiles indicates a steady rate of removal over time for all tested operational conditions, whereas the general trend suggests that the TiO_2 dose has a bigger impact than the UV intensity on DOC removal. The greater impact of dose over intensity is evidenced by a sharper reduction gradient in the removal profile and a higher overall removal observed for the TiO_2 doses of 5 g/L (60%) and 10 g/L (79%) under the UV intensity of 30 W/m^2.

Similarly distinctive trends were observed for the AeMBR effluent when exposed to different TiO_2 doses and UV intensities (Fig. 3b). These data series displayed a similar linearity to the AnMBR samples, indicating that a steady DOC removal rate was experienced over the 300 min experiment period. In the samples with 1 g/L and 2 g/L TiO_2 doses, the removal profiles exhibited a rapid decrease followed by stabilisation after reaching a removal of 80%. Indeed, stability was achieved with 1 g/L and 2 g/L TiO_2 doses regardless of the UV intensity, while the samples with 2 g/L dose required 120 min and the 1 g/L dosing samples took 180 min. This highlights a trade-off effect between the catalyst dosage and energy consumption during the treatment of the AeMBR effluent. However, a maximum DOC removal of 80% was observed for both MBR effluents regardless of the operational conditions, suggesting the potential presence of a recalcitrant fraction of organics or the adsorption sites were all covered with unreactive compounds. This may be caused by the colloid substances in the MBR effluents (Maghsoodi et al., 2019; Snow et al., 2019), as well as the nutrient compounds (Kim and Choi, 2002; Klare et al., 2000; Lee et al., 2016).

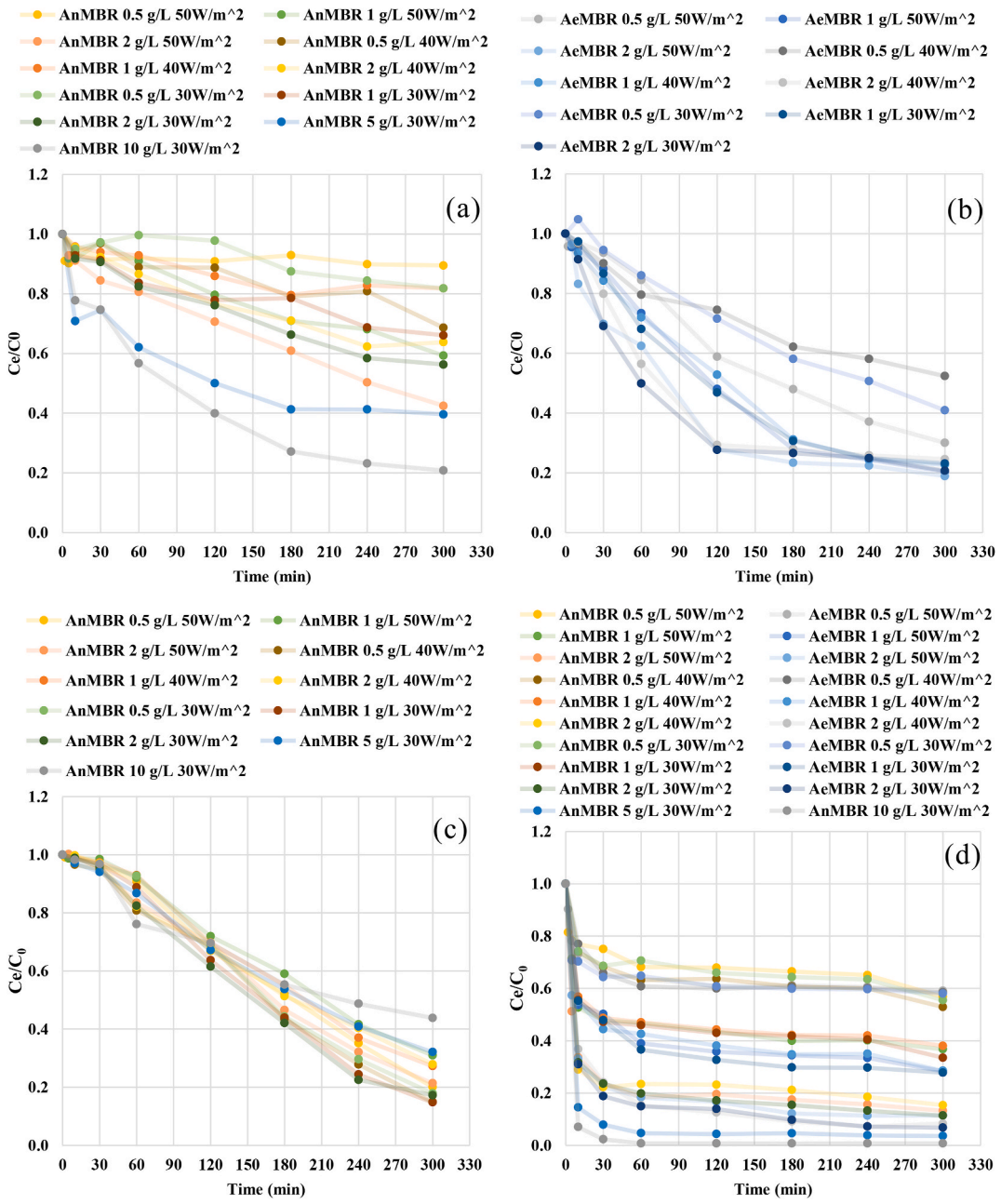

Fig. 3. Removal profiles in AnMBR (a-DOC, c-TN, d-TP) and AeMBR (b-DOC, d-TP) effluents by UV/TiO_2, where the value next to the legend is the correspondence TiO_2 dosing concentration and UV intensity.

The TN profiles for the photocatalysis of the AnMBR effluent displayed a similar shape (constant removal rate over time) for all tested conditions but exhibited a significant improvement on the removal rate constant (Fig. 3c). The average TN removal rate constant increased from 0.00025 min^{-1} to 0.0046 min^{-1}, this 1.5 log enhancement clearly demonstrates the benefit of the adsorption-photocatalytic process over monophonic adsorption. The overall removal percentage varies from 56% to 85% with a TiO_2 dosing amount from 0.5 g/L to 5 g/L, whereas the UV intensity was found to have a negligible effect on the removal rate and overall removal percentage. However, literature has shown the $OH^{\cdot}$ radicals can oxidize the ammonium to the forms of nitrite and nitrate in the pure ammonium solution, but suggested a very limited photodegradation by pure TiO_2 suspensions in a neutral pH condition (Lati et al., 1972; Murgia et al., 2005; Zhang et al., 2021). Indeed, we did not observe the formation of nitrite or nitrate in any trials. This agrees with Kim and Choi (2002) and Klare et al. (2000) that ammonium ions are not degraded under particular conditions similar to this paper, where the ammonium tend to be photodegradable as the fraction of ammonia at a pH of 11. Hence this suggests the removal of ammonia in our experiments was only by adsorption, and ultimately experiences a competing effect as for the phosphate. This therefore explains the lowest removal percentage was observed with the highest TiO_2 dose of 10 g/L, and the second lowest was the sample dosed with 5 g/L. This suggests the TiO_2 dosage in these two tests may have exceeded the optimum amount for the reactor and the overdose of TiO_2 has led to a substantial reduction in light penetration, which significantly decreases the photodegradation of organics hence much less adsorption site could be released. This ultimately resulted in a lower removal efficiency for organic and nitrogen (ammonium) compounds. However, the non-degradation of ammonia compounds highlights the potential selective removal by varying the UV intensity, and no further denitrification required since no nitrite or nitrate is generated, as well as a

promising insight of ammonia recovery during the regeneration of TiO_2.

All phosphate removal profiles displayed a short critical removal period regardless of the dosage, UV intensity and water matrix, whereas more than 90% of the phosphate was removed within 60 min with TiO_2 dosing of 5 and 10 g/L (Fig. 3d). The trends after the equilibrium point displayed a steady decrease but corresponding to a very limited removal percentage. Furthermore, the overall phosphate removal percentage displayed significant correlation to the TiO_2 dose, while again the UV intensity had a negligible impact. This agreed with the findings from the adsorption isotherm that a maximum adsorption capacity is achieved for phosphate.

The UV photocatalysis of the AeMBR effluent displayed a higher phosphate removal percentage in each sample compared to the percentage in AnMBR sample obtained with the same operational condition, which is different from the results observed without UV irradiation. This can be explained by a competing effect between the compounds which only adsorb and those which are photodegradable, and as the mineralization of degradable compounds release the adsorption site hence more phosphate can be adsorbed. The assistance of UV irradiation did slightly increase the overall removal rate for the 0.5, 1 and 2 g/L doses for both effluents but reduced in the AnMBR samples with 5 and 10 g/L doses. The reduced overall removal percentage observed with 5 and 10 g/L TiO_2 dose is respectively similar to the TN result for the same sample, as the overdose of TiO_2 reduces the light penetration. This confirmed the finding in the adsorption tests that a high TiO_2:N/P ratio may not be the optimum dosage if the nutrients removal is set for the higher priority than organic matter. However, the identified catalyst-energy trade-off effect suggests that once the TiO_2 dose exceeds a certain TiO_2:N/P ratio to ensure there is still enough capacity for photodegradable substance after the adsorption of ammonium and phosphate, an increase in TiO_2 dose can speed up the removal of DOC regardless of the UV intensity, shortening the time required to reach the same overall removal percentage.

3.2.2. Removal kinetics

As shown in Table 3, the feed water matrix and UV intensity were found to have negligible impact on the rate constant of total phosphorus, while the increasing TiO_2 dosing concentration had a significant increase on K_{TP}. However, the K_{TP} of the AnMBR samples with 5 g/L and 10 g/L TiO_2 dosing concentrations agreed with the finding from the adsorption isotherm that a limited increase in adsorption capacity was achieved once the adsorbent reached a certain ratio (Li et al., 2002), which in this study was TiO_2:TP weight ratio of 724:1. The removal profiles in Fig. 3 d exhibit a limited overall removal percentage and a limit removal after the equilibrium point, suggesting that the phosphorus present (as phosphate) can have a competing effect by adsorbing to TiO_2 at the start of the photocatalysis process but a negligible impact after reaching the equilibrium point in batch operation mode. However, if the system was operating in continuous mode, that phosphorus will not reach an equilibrium, therefore more phosphorus would be adsorbed until there is no capacity remaining on the TiO_2. In batch mode, phosphorus affects the UV/TiO_2 process by proportionally reducing the adsorption capacity and the available reactive surface for radical generation, which will ultimately reduce the overall efficiency of the photocatalysis process. Therefore, pre-removal of phosphorus from the MBR effluents can reduce the required dosage of TiO_2 and simultaneously increase the efficacy of the photocatalytic process for the degradation of organic matter, which may be beneficial to reduce the overall operational expenditure.

Table 3
Removal rate constant for TP under various UV intensities in AnMBR and AeMBR effluent.

TiO_2 dosage (g/L)	UV intensity (W/m^2)	AnMBR K_2 (min^{-1})	TiO_2:TP w/w	AeMBR K_2 (min^{-1})	TiO_2:TP w/w
0.5	30	0.2029	72:1	0.2113	96:1
	40	0.1875		0.2131	
	50	0.2115		0.2164	
1	30	0.2113	145:1	0.2441	192:1
	40	0.2131		0.2560	
	50	0.2164		0.2529	
2	30	0.3661	289:1	0.3755	383:1
	40	0.3874		0.3777	
	50	0.3777		0.3924	
5	30	0.8323	724:1	N/A	
10		0.7753	1447:1		

Note: N/A: Not available, w/w: weight-to-weight ratio.

As shown in Fig. 4, the K_{DOC} value for the AnMBR effluent was lower than the value for the AeMBR effluent under the sample operational conditions except the samples with a 0.5 g/L TiO_2 dose and 50 W/m^2 UV intensity. This helps explain the low overall removal observed in Fig. 3 for all AnMBR samples as they have much higher initial DOC concentrations compared to the AeMBR samples. This can be explained by the limited total adsorption capacity of TiO_2 under a low dosing concentration scenario. In this study the TiO_2:DOC for these samples were below 75:1. The explanatory mechanism here is that phosphate is taking the initial empty adsorption capacity, then continuously taking the released capacity after the degradation of organic compounds. Competition in the AnMBR effluent is more crucial since the ammonia was simultaneously following the pathway of adsorption, which ultimately leads to a reduction in the available photocatalysis area. Furthermore, the rate constant of K_{IC} was higher than K_{TC} in all AnMBR samples (Fig. 4a, b, c), whereas for the AeMBR samples, K_{TC} is higher than K_{IC} (Fig. 4d, e, f). Since the degradation mechanism of organic compounds by UV/TiO_2 is strongly dependent on the adsorption of the compounds (Maghsoodi et al., 2019; Snow et al., 2019), this validated the hypothesis that the other fraction of the TC, which contributes to DOC substances in this study, consists of lower MW compounds compared to the IC compounds in both effluents. Since the initial DOC and IC concentrations are much higher in the AnMBR effluent compared to those in the AeMBR effluent, the IC compounds with a higher MW experience a higher adsorption rate, resulting in a higher contact ratio with generated radicals (Carra et al., 2016), ultimately leading to a higher removal rate and consequently a lower K_{DOC} for the AnMBR. In comparison, in the AeMBR samples K_{TC} was consistently higher than K_{IC}, synchronously leading to a higher K_{DOC}. This additionally explains the faster DOC removal in AeMBR effluent compared to AnMBR.

In the sample taken at 0.5 g/L TiO_2 dose and 50 W/m^2 UV intensity, the K_{DOC} value (0.0046 min^{-1}) was much higher compared to two other AnMBR samples with 1 g/L (0.0017 min^{-1}) and 2 g/L (0.0029 min^{-1}) TiO_2 dosing concentration under the same UV intensity, while it is only slightly higher than the K_{DOC} value (0.0041 min^{-1}) of the AeMBR sample generated under the same operational condition. This was due to the fact observed in Fig. 4a, 5b and 5c that K_{DOC} was inversely proportional to K_{TN} in the AnMBR samples, indicating there might be a trade-off effect after the fast adsorption of phosphorus occurred between the removal of organic compounds and ammonia due to limited capacity of adsorption. The organic-ammonia trade-off effect was observed in samples obtained both with a fixed TiO_2 dosing concentration while varying the UV intensity and with a fixed UV intensity with various TiO_2 dosing concentrations. In Fig. 4 with a fixed UV intensity of 30 W/m^2, K_{TN} decreased with increasing dose, while in Fig. 4 c, the K_{DOC} decreased with increasing K_{TN} and dose at a UV intensity of 50 W/m^2. However, the removal mechanism is different between the samples displayed in Fig. 4a and Fig. 4c. This was due to the fact that in the particular conditions reported in this study, only DOC in the AnMBR effluent can be photocatalytically degraded. Therefore, the removal rate obtained during the UV/TiO_2 process involves the mechanisms of both adsorption and degradation for DOC, but only adsorption for the ammonia. In the samples exposed to 30 W/m^2 (Fig. 4a), the relatively lower UV intensity led to an adsorption dependent removal of DOC rather than photodegradation. To explain, at low TiO_2 doses (<1 g/L) the UV irradiation

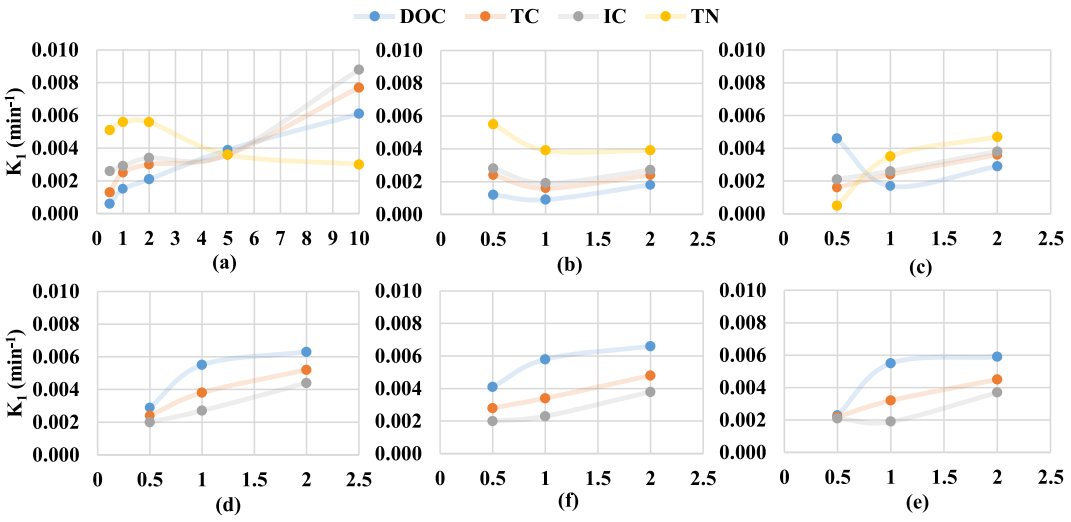

Fig. 4. UV/TiO_2 photocatalysis rate constant under various UV intensities in AnMBR (a-30 W/m^2, b-40 W/m^2, c-50 W/m^2) and AeMBR (d-30 W/m^2, e−40 W/m^2, f-50 W/m^2) effluent. Where the X-axis is the TiO_2 dosing concentration in g/L.

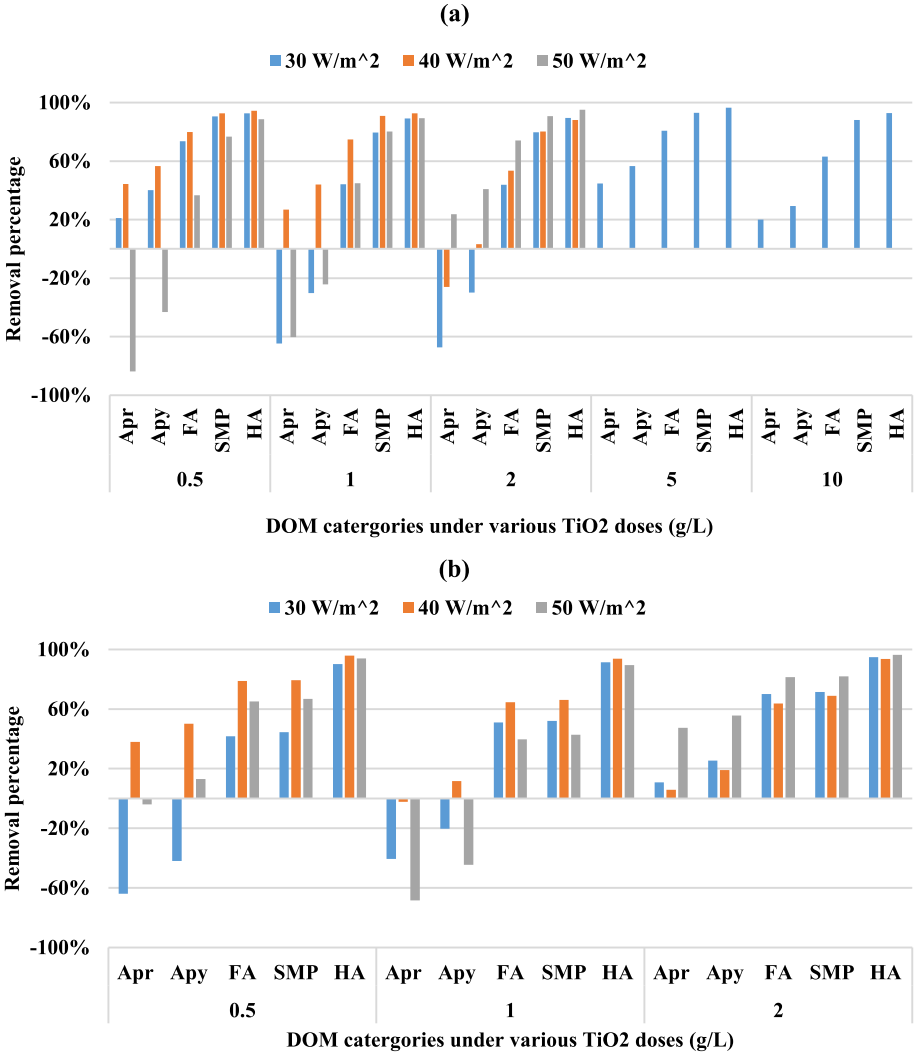

Fig. 5. DOM removal by UV/TiO_2 in AnMBR effluent (a) and AeMBR effluent (b) under various TiO_2 doses and UV intensities. Where: APr - aromatic protein tyrosine-like; APy - aromatic protein tryptophan-like; FA - fulvic acid-like; SMP - soluble microbial products; HA - humic acid-like.

offered a limited promotion of the degradation due to a lower adsorption capacity, therefore the competing effect between the nutrients and organics had led to a higher K_{TN} compared to K_{DOC}. Whilst in the samples treated with an increasing TiO_2 dosage from 1 g/L to 2 g/L, an increased capacity boosted the degradation of DOC and offered more adsorption capacity for both DOC and ammonia, which explains the increased K_{DOC} but constant K_{TN}. This also helps explaining the trend observed for the samples exposed to a UV intensity of 40 W/m^2, as the same trade-off effect between DOC and ammonia appeared as seen earlier in the samples exposed to 30 W/m^2. However, a further increase of the TiO_2 dosage (>5 g/L) shifted the adsorption priority from nutrients towards the DOC, which resulted in a significant increase and decrease for K_{DOC} and K_{TN}, respectively (Fig. 4a).

In contrast, assuming a similar adsorption scenario of DOC and ammonia in the samples exposed to 50 W/m^2 (Fig. 4c), increasing the UV intensity from 30 W/m^2 to 50 W/m^2 significantly promoted the photodegradation of DOC, as well as restricted the adsorption of ammonia with an increasing temperature (Rouquerol et al., 1999; Striolo et al., 2005), ultimately resulting in a much higher K_{DOC} compared to other samples and the lowest K_{TN} based on the organic-ammonia trade-off effect. However, the cross point between the 0.5 g/L and 1 g/L dosing concentration in Fig. 4 c may be the result of the competition effect discussed above, as the phosphate and ammonia took the released adsorption capacity whilst the degradation is much faster under a higher UV intensity, leading to a lower overall removal efficiency. This simultaneously explains the increased K_{DOC} and K_{TN} by increasing the TiO_2 dosage from 1 g/L to 2 g/L under the same 50 W/m^2 UV intensity. This performed as a co-effect of higher overall adsorption capacity and a faster degradation of DOC, creating much more adsorption capacity in comparison to samples that experienced a lower DOC degradation rate. Subsequently, this helps explain the different organic-ammonia trade-off trends observed between Fig. 4a and Fig. 4c since the adsorption rate and capacity of TN is not promoted by increasing the TiO_2 dose. Moreover, comparing the K_{DOC} and K_{TN} obtained at a fixed TiO_2 dosing concentration while varying UV intensity, increasing the UV intensity resulted in a reduction of K_{TN} but an increase of K_{DOC}. This suggests the adsorption of ammonia was less favoured than that of organic compounds by the increasing UV intensity. Therefore, this explains the similar overall DOC removal but a different removal rate constant observed for the AnMBR effluent treated by 5 g/L TiO_2 dose and 30 W/m^2 UV intensity (Fig. 3a) and with 2 g/L TiO_2 and 50 W/m^2 (Fig. 3c). This addresses the fundamental of the catalyst-energy trade-off effect which is linked to the adsorption-photodegradation trade-off effect, where similar removal efficiencies can be achieved by improving either of the adsorption and photodegradation processes.

The K_{DOC} obtained in the monophonic photocatalytic degradation of DOC in the AeMBR effluent was found to have more direct link to the operational conditions. But the increased TiO_2 dosage had limited impact in boosting the removal rate constant due to a low initial concentration of pollutants present in the AeMBR effluent.

The ineffectiveness of increasing the UV intensity in the high dose samples (>1 g/L) may be caused by a limitation in the experimental setup used for this study. Degradation only occurred at the surface of the solution, where the UV irradiation contacts the TiO_2, and the petri dish was therefore designed to have a large surface area to receive the UV irradiation from the lamps installed above. In the high dosage scenarios (where we observed that even the phosphate does not take all the absorption capacity) the overall available reacting surface area is too small due to the formed TiO_2 mask. This concomitantly leads to a limited effect through increasing the intensity of UV irradiation when a high TiO_2 dosing concentration is used. The increased removal rate found in higher TiO_2 dosing concentration samples was caused more by adsorption not degradation, which may also explain the cause of the adsorption-photodegradation trade-off effect found in AnMBR samples, as theoretically a higher K_{DOC} should be expected with the operational condition of 5 g/L and 30 W/m^2.

3.2.3. DOM removal

As DOC is a component of dissolved organic matter (DOM) (Moody and Worrall, 2017), monitoring the removal of DOM can also offer a more comprehensive view of the overall photocatalysis process, as well as a potential view of the variation of primary halogenated DBP precursors (Bond et al., 2011; Ma et al., 2016). Therefore, the removal percentage of each measured DOM fraction was calculated with the fluorescence integrated composition analysis results (Fig. 5).

The process of DOM fraction removal by UV/TiO_2 displayed non-selectivity with regard to each single type of DOM (Fig. 5) regardless of the effluent type (water matrix) and operational condition (TiO_2 dose and UV intensity). The AnMBR (Fig. 5a) and AeMBR (Fig. 5b) effluents displayed a similar response in terms of the different UV intensities, whilst a relatively similar removal percentage was observed between the two effluents when conducted with the same TiO_2 dosing concentrations. Both effluents displayed a significant removal of humic acid-like compounds (HA) (>89%) regardless of the operational condition. The removal percentage of each DOM category confirmed the adsorption mechanisms to follow in decreasing order of the MW, whereas the higher removal is matched with the higher DOM MW (Li et al., 2002; Lim et al., 2011). Moreover, the negative removal found for APr (tyrosine-like aromatic proteins) and APy (tryptophan-like aromatic proteins) in both effluents may suggest the aromatic protein-like substances could be the mineralization by-product of photocatalysis process. However, positive removal of Apr and APy was then observed with the higher dose for AnMBR (5 mg/L, 10 g/L) and AeMBR (2 g/L) tests, suggesting the generated by-product AP could be removed by either high UV intensities with sufficient adsorption capacity, or exceed amount of adsorption capacity provided by the high TiO_2 doses.

Under the optimal operational conditions such as 1 g/L and 40 W/m^2, with respect to achieving high DOM removal performance, a significant amount of HA and soluble microbial products (SMP) was removed by the UV/TiO_2 photocatalysis and a very low level of AP was observed in the permeate produced by both MBRs. This has led to a significant reduction of primary halogenated DBP precursors (Bond et al., 2011; Ma et al., 2016), which ultimately would lead to low DBP formation during the use of chlorine based pathogen control strategies for recycled water distribution (Capocelli and Piemonte, 2021). This is similar to the results reported by Gora and Andrews (2017) that TiO_2 photocatalysis can reduce the DBP formation potential of surface water with an treatment time over 30 min. Furthermore, AnMBR samples displayed a higher SMP removal compared to AeMBR. This was due to the non-selective removal of DOM while a high initial DOM concentration was present in the AnMBR effluent. In contrast, AeMBR samples exhibited a higher HA removal compared to the AnMBR. This agrees with Bekbolet (1996) and Wiszniowski et al. (2002) that under a fixed TiO_2 concentration, increasing the humic acid concentration drives a decrease of radical generation efficiency. This is because the HA substances can readily absorb the UV_{254} irradiation, leading to not only a lower removal of HA, but also a reduced overall photocatalysis efficiency (Carra et al., 2016; Maghsoodi et al., 2019; Snow et al., 2019). Hence the high amount of HA present in the AnMBR samples is significantly limiting the overall photodegradation efficiency.

3.3. Future perspective for UV/TiO_2 as post-treatment of MBR effluents

Due to the energy consumption of the UV lights, the costs of purchasing the catalyst (TiO_2), replacement due to losses in the process, and also filtering the TiO_2 out of the solution, UV/TiO_2 is considered an expensive and energy intensive processes. To illustrate, Al-Bastaki (2004) reported an energy use of about 4 kWh/m^3 for TiO_2/UV. However, the regenerable and solar-activatable characters of TiO_2 are seen as having the potential to overcome these limitations (Chatzisymeon et al., 2013; Loeb et al., 2019; MacAdam et al., 2012). The complex matrix and high concentrations of organics and nutrients in AnMBR effluents constitute limitations for the use of UV/TiO_2 as a single barrier to secure

a water quality sufficient for many reuse applications. The non-photodegradation of the adsorbed ammonia leading to competition for adsorption on the media raise the question if the ammonia should be removed before the UV/TiO_2 process. If keeping the ammonia in the water, the organic-ammonia trade-off effect suggests that by optimising the intensity of UV irradiation, UV/TiO_2 can provide a selective solution for organic or ammonia prioritised removal for the post-treatment of AnMBR effluent. However, this highlights the need for research to potentially recover the adsorbed ammonia during a regeneration of TiO_2. On the other hand, this can be offset with replacing the pure TiO_2 with metal loaded ones such as TiO_2/Pt, that with the presence of Pt the adsorbed ammonia can be oxidized to a final product of N_2H_2 (Lee et al., 2002; Yuzawa et al., 2012), ultimately forming Nitrogen gas due to the self-decomposition under ambient temperature and pressure (Zhang et al., 2021). However, by removing the phosphorus and potentially ammonia as well, this would significantly address the competing effect between the nutrients with organic compounds, which is beneficial to achieve the full photocatalytic proficiency of TiO_2. Ideally TiO_2 can be used as an eternal catalyst without adsorbing the phosphorus and ammonia. In this regard, AnMBR technologies will need an extra post-treatment step but have potential for ammonia and phosphate recovery (Lee et al., 2016; Song et al., 2018b; Xie et al., 2016). With the AeMBR, anaerobic and anoxic stages can be combined with the oxic stage to remove the nitrogen (nitrate) and phosphorus by biological processes. The catalyst-energy trade-off effect then can be used to optimise the operational conditions, reducing the operational cost of implemented schemes. In general, developments in reactor design (Dai et al., 2013; Natarajan et al., 2011) are beneficial to enhance the UV transmission efficiency regardless of the effluent matrix, which can ultimately improve the overall photocatalysis performance. Therefore, by tackling the current weaknesses, UV/TiO_2 can be a promising post-treatment solution for the AnMBR effluent, specifically when facing the challenge from emerging contaminants (Carra et al., 2015, 2016; Fattahi et al., 2021; Kanakaraju et al., 2018) in modern water reuse applications.

4. Conclusion

In this study, the first direct comparison of UV/TiO_2 photocatalysis for the post-treatment of AnMBR and AeMBR treating real municipal wastewater was conducted focusing on the removal performance of organics and nutrients (nitrogen and phosphorus). Results show that the nutrients present in the effluent, in particular phosphorus and ammonia in the AnMBR effluent, are adsorbed onto the media but not degraded. The removal mechanisms in both effluents are then identified as adsorption for the organic, ammonia and phosphorus, but only photodegradation for the organic compounds. Removals of the organics of up to 80%, was achieved for both effluents, demonstrating good performance and the potential to achieve low levels for reuse. However, the competing effect between the nutrients and organic compounds is expected to lead to deterioration of the performance over time as the adsorption sites are saturated by nutrients. As such, a greater impact of the TiO_2 dosing concentration than the UV intensity was observed on the overall removal performance, particularly more crucial with the presence of ammonia in the AnMBR effluent. With mitigations such as advancement on the reactor design and pre-treatment of the nutrients, UV/TiO_2 photocatalysis can achieve a prioritised removal of organic matter or nutrients for AnMBR effluent for reuse.

CRediT authorship contribution statement

Yu Huang: Conceptualization, Data curation, Investigation, Methodology, Writing – original draft, Writing – review & editing. **Paul Jeffrey:** Conceptualization, Resources, Supervision, Writing – review & editing. **Marc Pidou:** Conceptualization, Project administration, Supervision, Writing – review & editing.

Declaration of competing interest

The authors declare that they have no known competing financial interests or personal relationships that could have appeared to influence the work reported in this paper.

Data availability

Data will be made available on request.

Appendix A. Supplementary data

Supplementary data to this article can be found online at https://doi.org/10.1016/j.jenvman.2024.120628.

References

Al-Bastaki, N.M., 2004. Performance of advanced methods for treatment of wastewater: UV/TiO2, RO and UF. Chem. Eng. Process. Process Intensif. 43, 935–940. https://doi.org/10.1016/j.cep.2003.08.003.

Atalay, S., Ersöz, G., 2020. Hybrid application of advanced oxidation processes to dyes' removal. In: Sharma, S.K.B.T. (Ed.), Green Chemistry and Water Remediation: Research and Applications. Elsevier, pp. 209–238. https://doi.org/10.1016/B978-0-12-817742-6.00007-4. G.C. and W.R.R. and A.

Augsburger, N., Zaouri, N., Cheng, H., Hong, P.Y., 2021. The use of UV/H2O2 to facilitate removal of emerging contaminants in anaerobic membrane bioreactor effluents. Environ. Res. 198, 110479 https://doi.org/10.1016/j.envres.2020.110479.

Azeez, F., Al-Hetlani, E., Arafa, M., Abdelmonem, Y., Nazeer, A.A., Amin, M.O., Madkour, M., 2018. The effect of surface charge on photocatalytic degradation of methylene blue dye using chargeable titania nanoparticles. Sci. Rep. 8, 7104. https://doi.org/10.1038/s41598-018-25673-5.

Bekbolet, M., 1996. Destructive removal of humic acids in aqueous media by photocatalytic oxidation with illuminated titanium dioxide. J. Environ. Sci. Heal. - Part A Toxic/Hazardous Subst. Environ. Eng. 31, 845–858. https://doi.org/10.1080/10934529609376392.

Benitez, F.J., Acero, J.L., Real, F.J., Roldan, G., Casas, F., 2011. Comparison of different chemical oxidation treatments for the removal of selected pharmaceuticals in water matrices. Chem. Eng. J. 168, 1149–1156. https://doi.org/10.1016/j.cej.2011.02.001.

Benkoula, S., Sublemontier, O., Patanen, M., Nicolas, C., Sirotti, F., Naitabdi, A., Gaie-Levrel, F., Antonsson, E., Aureau, D., Ouf, F.X., Wada, S.I., Etcheberry, A., Ueda, K., Miron, C., 2015. Water adsorption on TiO2 surfaces probed by soft X-ray spectroscopies: bulk materials vs. isolated nanoparticles. Sci. Rep. 5, 15088 https://doi.org/10.1038/srep15088.

Bond, T., Goslan, E.H., Parsons, S.A., Jefferson, B., 2011. Treatment of disinfection by-product precursors. Environ. Technol. 32, 1–25. https://doi.org/10.1080/09593330.2010.495138.

Capocelli, M., Piemonte, V., 2021. Technologies for Water Reuse: Current Status and Future Challenges.

Carra, I., Sánchez Pérez, J.A., Malato, S., Autin, O., Jefferson, B., Jarvis, P., 2016. Performance of different advanced oxidation processes for tertiary wastewater treatment to remove the pesticide acetamiprid. J. Chem. Technol. Biotechnol. 91, 72–81. https://doi.org/10.1002/jctb.4577.

Carra, I., Sánchez Pérez, J.A., Malato, S., Autin, O., Jefferson, B., Jarvis, P., 2015. Application of high intensity UVC-LED for the removal of acetamiprid with the photo-Fenton process. Chem. Eng. J. 264, 690–696. https://doi.org/10.1016/j.cej.2014.11.142.

Chatzisymeon, E., Foteinis, S., Mantzavinos, D., Tsoutsos, T., 2013. Life cycle assessment of advanced oxidation processes for olive mill wastewater treatment. J. Clean. Prod. 54, 229–234. https://doi.org/10.1016/j.jclepro.2013.05.013.

Chen, X., Guo, J., Xie, G.J., Liu, Y., Yuan, Z., Ni, B.J., 2015. A new approach to simultaneous ammonium and dissolved methane removal from anaerobic digestion liquor: a model-based investigation of feasibility. Water Res. 85, 295–303. https://doi.org/10.1016/j.watres.2015.08.046.

CNEPA, 2021. Water Reuse Guildlines GB/T 41016-17-18 2021.

Crone, B.C., Garland, J.L., Sorial, G.A., Vane, L.M., 2016. Significance of dissolved methane in effluents of anaerobically treated low strength wastewater and potential for recovery as an energy product: a review. Water Res. 104, 520–531. https://doi.org/10.1016/j.watres.2016.08.019.

Dai, K., Lu, L., Dawson, G., 2013. Development of UV-LED/TiO2 device and their application for photocatalytic degradation of methylene blue. J. Mater. Eng. Perform. 22, 1035–1040. https://doi.org/10.1007/s11665-012-0344-7.

Dolejs, P., Ozcan, O., Bair, R., Ariunbaatar, J., Bartacek, J., Lens, P.N.L., Yeh, D.H., 2017. Effect of psychrophilic temperature shocks on a gas-lift anaerobic membrane bioreactor (Gl-AnMBR) treating synthetic domestic wastewater. J. Water Process Eng. 16, 108–114. https://doi.org/10.1016/j.jwpe.2016.12.005.

Domingos, R.F., Peyrot, C., Wilkinson, K.J., 2010. Aggregation of titanium dioxide nanoparticles: role of calcium and phosphate. Environ. Chem. 7, 61–66. https://doi.org/10.1071/EN09110.

Fattahi, A., Jaciw-Zurakowsky, I., Srikanthan, N., Bragg, L., Liang, R., Zhou, N., Servos, M., Arlos, M., 2021. Effect of background water matrices on pharmaceutical and personal care product removal by uv-led/tio2. Catalysts 11, 576. https://doi.org/10.3390/catal11050576.

Finkbeiner, P., Redman, J., Patriarca, V., Moore, G., Jefferson, B., Jarvis, P., 2018. Understanding the potential for selective natural organic matter removal by ion exchange. Water Res. 146, 256–263. https://doi.org/10.1016/j.watres.2018.09.042.

Foglia, A., Cipolletta, G., Frison, N., Sabbatini, S., Gorbi, S., Eusebi, A.L., Fatone, F., 2019. Anaerobic membrane bioreactor for urban wastewater valorisation: operative strategies and fertigation reuse. Chem. Eng. Trans. 74, 247–252. https://doi.org/10.3303/CET1974042.

Gora, S.L., Andrews, S.A., 2017. Adsorption of natural organic matter and disinfection byproduct precursors from surface water on TiO2 Nanoparticles: pH effects, isotherm modelling and implications for using TiO2 for drinking water treatment. Chemosphere 174, 363–370. https://doi.org/10.1016/j.chemosphere.2017.01.125.

Halimi, S.U., Abu Bakar, N.F., Ismail, S.N., Hashib, S.A., Naim, M.N., 2014. Electrospray deposition of titanium dioxide (TiO2) nanoparticles. AIP Conf. Proc. 1586, 57–62. https://doi.org/10.1063/1.4866730.

Harb, M., Hong, P.Y., 2017. Anaerobic membrane bioreactor effluent reuse: a review of microbial safety concerns. Fermentation 3. https://doi.org/10.3390/fermentation3030039.

Huang, Y., Jeffrey, P., Pidou, M., 2023. Municipal wastewater treatment with anaerobic membrane Bioreactors for non-potable reuse: a review. Crit. Rev. Environ. Sci. Technol. 1–23. https://doi.org/10.1080/10643389.2023.2279886.

Huang, Y., Jeffrey, P., Pidou, M., 2022. A comparative evaluation of reverse osmosis membrane performance when combined with anaerobic or aerobic membrane bioreactors for indirect potable reuse applications. J. Water Process Eng. 50, 103295 https://doi.org/10.1016/j.jwpe.2022.103295.

ISO, 2018. Water reuse in urban areas. Guidelines for water reuse safety evaluation. Assessment parameters and methods. Standard 20761.

Janssens, R., Cristovao, M.B., Bronze, M.R., Crespo, J.G., Pereira, V.J., Luis, P., 2019. Coupling of nanofiltration and UV, UV/TiO2 and UV/H2O2 processes for the removal of anti-cancer drugs from real secondary wastewater effluent. J. Environ. Chem. Eng. 7, 103351 https://doi.org/10.1016/j.jece.2019.103351.

Kanakaraju, D., Glass, B.D., Oelgemöller, M., 2018. Advanced oxidation process-mediated removal of pharmaceuticals from water: a review. J. Environ. Manag. 219, 189–207. https://doi.org/10.1016/j.jenvman.2018.04.103.

Kim, S., Choi, W., 2002. Kinetics and mechanisms of photocatalytic degradation of (CH3)nNH4-n+ ($0 \leq n \leq 4$) in TiO2 suspension: the role of OH radicals. Environ. Sci. Technol. 36, 2019–2025. https://doi.org/10.1021/es015560s.

Klare, M., Scheen, J., Vogelsang, K., Jacobs, H., Broekaert, J.A.C., 2000. Degradation of short-chain alkyl- and alkanolamines by TiO2- and Pt/TiO2-assisted photocatalysis. Chemosphere 41, 353–362. https://doi.org/10.1016/S0045-6535(99)00447-6.

Lati, J., Meyerstein, D., Lati, J., Meyerstein, D., 1972. Trivalent Nickel. I. A pulse radiolytic study of the formation and decomposition of the ammoniacal complex in aqueous solution. Inorg. Chem. 11, 2393–2397. https://doi.org/10.1021/ic50116a020.

Lazarova, V., 2015. Milestones in water reuse: the best success stories. Milestones Water Reuse Best Success Stories. https://doi.org/10.2166/9781780400716.

Lee, J., Park, H., Choi, W., 2002. Selective photocatalytic oxidation of NH3 to N2 on platinized TiO2 in water. Environ. Sci. Technol. 36, 5462–5468. https://doi.org/10.1021/es025930s.

Lee, K., Jutidamrongphan, W., Lee, S., Park, K.Y., 2016. Adsorptive removal of phosphate from wastewater using mesoporous titanium oxide. Adv. Civil, Envrionmental, Mater. 193, 470–482. https://doi.org/10.1016/j.jenvman.2017.02.030.

Levchuk, I., Sillanpää, M., 2020. Titanium dioxide-based nanomaterials for photocatalytic water treatment. In: Sillanpää, M. (Ed.), Advanced Water Treatment: Advanced Oxidation Processes. Elsevier, pp. 1–56. https://doi.org/10.1016/B978-0-12-819225-2.00001-6.

Li, F., Yuasa, A., Ebie, K., Azuma, Y., Hagishita, T., Matsui, Y., 2002. Factors affecting the adsorption capacity of dissolved organic matter onto activated carbon: modified isotherm analysis. Water Res. 36, 4592–4604. https://doi.org/10.1016/S0043-1354(02)00174-4.

Li, W., Xu, E., Schlenk, D., Liu, H., 2018. Cyto- and geno-toxicity of 1,4-dioxane and its transformation products during ultraviolet-driven advanced oxidation processes. Environ. Sci. Water Res. Technol. 4, 1213–1218. https://doi.org/10.1039/c8ew00107c.

Li, Y., Sun, S., Ma, M., Ouyang, Y., Yan, W., 2008. Kinetic study and model of the photocatalytic degradation of rhodamine B (RhB) by a TiO2-coated activated carbon catalyst: effects of initial RhB content, light intensity and TiO2 content in the catalyst. Chem. Eng. J. 142, 147–155. https://doi.org/10.1016/j.cej.2008.01.009.

Lim, T.T., Yap, P.S., Srinivasan, M., Fane, A.G., 2011. TiO2/AC composites for synergistic adsorption-photocatalysis processes: present challenges and further developments for water treatment and reclamation. Crit. Rev. Environ. Sci. Technol. 41, 1173–1230. https://doi.org/10.1080/10643380903488664.

Loeb, S.K., Alvarez, P.J.J., Brame, J.A., Cates, E.L., Choi, W., Crittenden, J., Dionysiou, D. D., Li, Q., Li-Puma, G., Quan, X., Sedlak, D.L., David Waite, T., Westerhoff, P., Kim, J. H., 2019. The Technology horizon for photocatalytic water treatment: sunrise or sunset? Environ. Sci. Technol. 53, 2937–2947. https://doi.org/10.1021/acs.est.8b05041.

Lofrano, G., Libralato, G., Casaburi, A., Siciliano, A., Iannece, P., Guida, M., Pucci, L., Dentice, E.F., Carotenuto, M., 2018. n.d.. Municipal wastewater spiramycin removal by conventional treatments and heterogeneous photocatalysis. Science of the Total Environment 624, 461–469. https://doi.org/10.1016/j.scitotenv.2017.12.145.

Ma, D., Xia, C., Gao, B., Yue, Q., Wang, Y., 2016. C-, N-DBP formation and quantification by differential spectra in MBR treated municipal wastewater exposed to chlorine and chloramine. Chem. Eng. J. 291, 55–63. https://doi.org/10.1016/j.cej.2016.01.091.

MacAdam, J., Ozgencil, H., Autin, O., Pidou, M., Temple, C., Parsons, S., Jefferson, B., 2012. Incorporating biodegradation and advanced oxidation processes in the treatment of spent metalworking fluids. Environ. Technol. 33, 2741–2750. https://doi.org/10.1080/09593330.2012.678389.

Maghsoodi, M., Jacquin, C., Teychené, B., Heran, M., Tarabara, V.V., Lesage, G., Snow, S. D., 2019. Emerging investigator series: photocatalysis for MBR effluent post-treatment: assessing the effects of effluent organic matter characteristics. Environ. Sci. Water Res. Technol. 5, 482–494. https://doi.org/10.1039/c8ew00734a.

Mangalgiri, K.P., Patton, S., Wu, L., Xu, S., Ishida, K.P., Liu, H., 2019. Optimizing potable water reuse systems: chloramines or hydrogen peroxide for UV-based advanced oxidation process? Environ. Sci. Technol. 53, 13323–13331. https://doi.org/10.1021/acs.est.9b03062.

Markovits, A., Ahdjoudj, J., Minot, C., 1996. A theoretical analysis of NH3 adsorption on TiO2. Surf. Sci. 365, 649–661. https://doi.org/10.1016/0039-6028(96)00753-4.

Moody, C.S., Worrall, F., 2017. Modeling rates of DOC degradation using DOM composition and hydroclimatic variables. J. Geophys. Res. Biogeosciences 122, 1175–1191. https://doi.org/10.1002/2016JG003493.

Murgia, S.M., Poletti, A., Selvaggi, R., 2005. Photocatalytic degradation of high ammonia concentration water solutions by TiO2. Ann. Chim. 95, 335–343. https://doi.org/10.1002/adic.200590038.

Natarajan, T.S., Thomas, M., Natarajan, K., Bajaj, H.C., Tayade, R.J., 2011. Study on UV-LED/TiO2 process for degradation of Rhodamine B dye. Chem. Eng. J. 169, 126–134. https://doi.org/10.1016/j.cej.2011.02.066.

Ojobe, B., Zouzelka, R., Satkova, B., Vagnerova, M., Nemeskalova, A., Kuchar, M., Bartacek, J., Rathousky, J., 2021. Photocatalytic removal of pharmaceuticals from greywater. Catalysts 11. https://doi.org/10.3390/catal11091125.

Pidou, M., Parsons, S.A., Raymond, G., Jeffrey, P., Stephenson, T., Jefferson, B., 2009. Fouling control of a membrane coupled photocatalytic process treating greywater. Water Research 43 (16), 3932–3939. https://doi.org/10.1016/j.watres.2009.05.030.

Rebelo, A., Farabegoli, G., Andreotti, F., Malo, A.P., Bonnici, P.G., Grima, G., Hickey, P., Tomazevic, E., Topkaya, P., Tunen, R. Van, Balmer, J., Vella, M., Van Tunen, R., Gunput, S., Perikenti, S., Ece, P., 2018. Report on urban water reuse. Eur. Union Netw. Implement. Enforc. Environ. Law 2 (0), 1–77.

Rouquerol, F., Rouquerol, J., Sing, K., 1999. Adsorption at the liquid–solid interface: thermodynamics and methodology. In: Rouquerol, F., Rouquerol, J., Sing, K.B.T.-A. by P., P, S. (Eds.), Adsorption by Powders and Porous Solids. Academic Press, London, pp. 117–163. https://doi.org/10.1016/b978-012598920-6/50006-3.

Rivero, M.J., Parsons, S.A., Jeffrey, P., Pidou, M., Jefferson, B., 2006. Membrane chemical reactor (MCR) combining photocatalysis and microfiltration for grey water treatment Water. Science and Technology 53 (3), 173–180. https://doi.org/10.2166/wst.2006.090.

Salgot, M., Folch, M., 2018. Wastewater treatment and water reuse. Curr. Opin. Environ. Sci. Heal. 2, 64–74. https://doi.org/10.1016/j.coesh.2018.03.005.

Shin, C., Bae, J., 2018. Current status of the pilot-scale anaerobic membrane bioreactor treatments of domestic wastewaters: a critical review. Bioresour. Technol. 247, 1038–1046. https://doi.org/10.1016/j.biortech.2017.09.002.

Shin, C., Szczuka, A., Jiang, R., Mitch, W.A., Criddle, C.S., 2021. Optimization of reverse osmosis operational conditions to maximize ammonia removal from the effluent of an anaerobic membrane bioreactor. Environ. Sci. Water Res. Technol. 7, 739–747. https://doi.org/10.1039/d0ew01112f.

Snow, S.D., LaRoy, C.E.L., Tarabara, V.V., 2019. Photocatalysis in membrane bioreactor effluent: assessment of inhibition by dissolved organics. J. Environ. Eng. 145, 06019001 https://doi.org/10.1061/(asce)ee.1943-7870.0001504.

Song, X., Luo, W., Hai, F.I., Price, W.E., Guo, W., Ngo, H.H., Nghiem, L.D., 2018a. Resource recovery from wastewater by anaerobic membrane bioreactors: opportunities and challenges. Bioresour. Technol. 270, 669–677. https://doi.org/10.1016/j.biortech.2018.09.001.

Song, X., Luo, W., McDonald, J., Khan, S.J., Hai, F.I., Price, W.E., Nghiem, L.D., 2018b. An anaerobic membrane bioreactor – membrane distillation hybrid system for energy recovery and water reuse: removal performance of organic carbon, nutrients, and trace organic contaminants. Sci. Total Environ. 628–629, 358–365. https://doi.org/10.1016/j.scitotenv.2018.02.057.

Striolo, A., Gubbins, K.E., Gruszkiewicz, M.S., Cole, D.R., Simonson, J.M., Chialvo, A.A., Cummings, P.T., Burchell, T.D., More, K.L., 2005. Effect of temperature on the adsorption of water in porous carbons. Langmuir 21, 9457–9467. https://doi.org/10.1021/la051120t.

Suzuki, H., Araki, S., Yamamoto, H., 2015. Evaluation of advanced oxidation processes (AOP) using O3, UV, and TiO2 for the degradation of phenol in water. J. Water Process Eng. 7, 54–60. https://doi.org/10.1016/j.jwpe.2015.04.011.

Tang, C.Y., Yang, Z., Guo, H., Wen, J.J., Nghiem, L.D., Cornelissen, E., 2018. Potable water reuse through advanced membrane Technology. Environ. Sci. Technol. 52, 10215–10223. https://doi.org/10.1021/acs.est.8b00562.

Thomas, A.G., Syres, K.L., 2012. Adsorption of organic molecules on rutile TiO2 and anatase TiO2 single crystal surfaces. Chem. Soc. Rev. 41, 4207–4217. https://doi.org/10.1039/c2cs35057b.

Tsoukleris, D.S., Gatou, M.-A., Lagopati, N., Sygellou, L., Christodouleas, D.C., Falaras, P., Pavlatou, E.A., 2023. Chemically Modified TiO2 Photocatalysts as an Alternative Disinfection Approach for Municipal Wastewater Treatment Plant Effluents Water. (Switzerland) 15 (11), 2052. https://doi.org/10.3390/w15112052.

USEPA, 2017. Potable Reuse Compendium.

USEPA, 2012. EPA Guidelines for Water Reuse U.S. Environmental Protection Agency, Guidelines for Water Reuse.

Venkiteswaran, J.J., Schiff, S.L., Ingalls, B.P., 2019. Quantifying the fate of wastewater nitrogen discharged to a Canadian river. Facets 4, 315–335. https://doi.org/10.1139/facets-2018-0028.

Villegas-Guzman, P., Silva-Agredo, J., Florez, O., Giraldo-Aguirre, A.L., Pulgarin, C., Torres-Palma, R.A., 2017. Selecting the best AOP for isoxazolyl penicillins degradation as a function of water characteristics: effects of pH, chemical nature of additives and pollutant concentration. J. Environ. Manag. 190, 72–79. https://doi.org/10.1016/j.jenvman.2016.12.056.

Wiszniowski, J., Robert, D., Surmacz-Gorska, J., Miksch, K., Weber, J.V., 2002. Photocatalytic decomposition of humic acids on TiO2. Part I: discussion of adsorption and mechanism. J. Photochem. Photobiol. Chem. 152, 267–273. https://doi.org/10.1016/S1010-6030(02)00022-9.

Xie, M., Shon, H.K., Gray, S.R., Elimelech, M., 2016. Membrane-based processes for wastewater nutrient recovery: Technology, challenges, and future direction. Water Res. 89, 210–221. https://doi.org/10.1016/j.watres.2015.11.045.

Yuzawa, H., Mori, T., Itoh, H., Yoshida, H., 2012. Reaction mechanism of ammonia decomposition to nitrogen and hydrogen over metal loaded titanium oxide photocatalyst. J. Phys. Chem. C 116, 4126–4136. https://doi.org/10.1021/jp209795t.

Zhang, G., Ruan, J., Du, T., 2021. Recent advances on photocatalytic and electrochemical oxidation for ammonia treatment from water/wastewater. ACS ES&T Eng. 1, 310–325. https://doi.org/10.1021/acsestengg.0c00186.